Shear lag analysis in reinforced concrete

Autor(en): **Ghani Razaqpur, A. / Ghali, Amin**

Objekttyp: **Article**

Zeitschrift: **IABSE reports of the working commissions = Rapports des commissions de travail AIPC = IVBH Berichte der Arbeitskommissionen**

Band (Jahr): **34 (1981)**

PDF erstellt am: **26.05.2024**

Persistenter Link: https://doi.org/10.5169/seals-26923

Shear Lag Analysis in Reinforced Concrete

Analyse du phénomène de flux du cisaillement (shear lag)

Schubversatz im Stahlbeton

A. GHANI RAZAQPUR
Graduate Student
University of Calgary
Canada

AMIN GHALI
Professor of Civil Engineering
University of Calgary
Canada

SUMMARY
At the intersection of the web of a T-beam or a box girder with the flange or with the top and bottom slabs longitudinal shear and transverse bending stresses occur. The finite element method of analysis is used to study the deformation and strength of reinforced and transversely prestressed concrete flanges under this stress condition. The analytical and experimental results are compared for beams tested in Zurich, Switzerland. The adequacy of the mathematical model to represent the behaviour of cracked reinforced concrete is assessed with particular attention to the shear lag phenomenon.

RÉSUMÉ
A la jonction de l'âme et de la table d'une poutre à caissons, des tensions de cisaillement longitudinal et de flexion transversale apparaissent. La méthode des éléments finis est utilisée pour étudier la déformation et la résistance de ces tables en béton armé à précontrainte transversale, soumises à ces conditions de charges. Les résultats analytiques et expérimentaux sont comparés sur base d'essais exécutés à Zurich (Suisse). La capacité du modèle mathématique de représenter le comportement du béton armé fissuré est analysée avec une attention toute spéciale au phénoméne de flux du cisaillement.

ZUSAMMENFASSUNG
Am Stoss des Steges eines T-Trägers oder eines Kastenträgers mit dem Flansch oder der Bodenplatte entstehen Längsschub- un Querbiegespannungen. Die Finite-Elemente-Methode ist auf diesen Fall angewandt. Theoretische und experimentelle Ergebnisse (aus Zürich) wurden verglichen, wobei gute Übereinsstimmung im Hinblick auf Schubversatz erzielt wurde.

1. INTRODUCTION

The successful application of the finite element method to the analysis of concrete structures depends much upon the development of accurate analytical models that can simulate the complex behaviour of concrete under multiaxial stresses, the initiation and propagation of cracks, bond and slip, and the manner in which stresses are subsequently transferred across cracks. Some of these problems have been successfully dealt with while others remain to be yet fully explored. Perhaps the most complex of these is the formulation of an acceptable shear transfer model.

An exact analysis of shear by finite element is indeed complex since an accurate modelling of most of the aforementioned phenomena is necessary. However, despite the complex nature of the problem, it is possible to obtain a fairly acurate picture of the overall stress condition by a rather simple model in most practical situations. Several investigators [1, 7, 13, 16] have used such simplified models to study the problem of shear in ordinary beams, deep beams, and panels.

In this paper yet another case of shear transfer is considered, namely the longitudinal shear at the web-flange connection of a flanged beam, and the interaction of this shear with transverse bending of the flange. In practice, this stress condition occurs at the connection of floor slabs with their supporting beams, between bridge decks and supporting girders, and at the connection of the webs and top and bottom slabs of box girders. Using a simplified shear model, four reinforced concrete T-beams that have been previously tested [2, 3, 4, 5] are analyzed by the finite element method. The model adopted is equally applicable to box girders but since no sufficiently documented test results are available for comparison with analytical findings, the results for T-beams only are compared here. The limitations of the applied simplified model and a review of some of the other proposed models is presented.

The purpose of comparing experimental and analytical results in this paper is to establish a procedure for the analysis of shear transfer at the web-flange connection which can be reliaby applied to situations not yet tested.

2. FINITE ELEMENT MODELLING

The program FELARC [11, 12] used in this investigation utilizes layered F.E. with an incremental iterative tangent stiffness approach. The concrete and distributed steel are represented by a quadrilateral inplane element QLC3 [18] with twelve nodal degrees of freedom and a quadrilateral plate bending element RBE [21] also with twelve degrees of freedom. The above two elements are combined to develop a shell element. The thickness is divided into a number of concrete and smeared steel layers, or prestressing layers, and the contribution of each is summed up to compute the element stiffness. Individual heavier bars or prestressing tendons are modelled by a so-called element bar which assumes perfect bond between the steel and concrete and which can be located anywhere within an element. The contribution of these bars to the element stiffness is directly superimposed on the element stiffness matrix.

3. CONSTITUTIVE MATERIAL RELATION

Increments of stress $\{\Delta\sigma\}$ and strain $\{\Delta\varepsilon\}$ in principal stress directions 1 and 2 are related by

$$\{\Delta\sigma\} = [D]\ \{\Delta\varepsilon\}$$

where [D] is the constitutive matrix shown in Eq. (1).

$$[D] = \frac{1}{1-\nu 2}\begin{bmatrix} E_1 & \nu\sqrt{E_1E_2} & 0 \\ \nu\sqrt{E_1E_2} & E_2 & 0 \\ 0 & 0 & \frac{1}{4}(E_2 + E_2 - 2\nu\sqrt{E_1E_2}) \end{bmatrix} \quad (1)$$

in which E_1 and E_2 are the uniaxial tangent moduli and ν is the Poisson's ratio. The values of E_1 and E_2 depend upon the ratio of the two principal stresses following the "equivalent uniaxial strain" concept of Darwin and Pecknold [9].

The equivalent stress-strain relationship employed to determine E_1 and E_2 is comprised of two parts, as illustrated in Fig. 1. Part I follows Eq. (2) proposed by Saenz [17],

$$\sigma = \frac{E_o\varepsilon}{(1 + \frac{E_o}{E_{cs}} - 2)(\frac{\varepsilon}{\varepsilon_{cu}}) + (\frac{\varepsilon}{\varepsilon_{cu}})^2} \quad (2)$$

whereas Part II traces the Smith-Young [20] model as described by Eq. (3),

$$\sigma = \sigma_c(\frac{\varepsilon}{\varepsilon_{cu}})\ \exp(1 - \frac{\varepsilon}{\varepsilon_{cu}}) \quad (3)$$

In the above equations, E_o, E_{cs}, σ_c and ε_{cu} are initial elastic modulus, secant modulus, maximum compressive stress, and the strain corresponding to σ_c, respectively (Fig. 1); σ and ε are equivalent uniaxial stress and strain [9].

The maximum compressive strength σ_c is determined from the modified biaxial failure envelope of Kupfer and Gerstle [14], and ε_{cu} is evaluated as a function of σ_c/f'_c, where f'_c is the uniaxial compressive cylinder strength. To avoid numerical difficulties, the value of the tangent modulus for the unloading portion of Fig. 1 is set equal to zero.

Steel and prestressing steel are both modelled as bilinear elastic-strain hardening material, including the Bauschinger effect.

4. CRACKING AND TENSION STIFFENING

In this study the smeared crack approach is adopted. When a principal stress exceeds the uniaxial tensile strength of concrete in a principal direction, cracking is assumed perpendicular to the particular direction. If $\sigma_1 \geq f'_t$, where f'_t is the uniaxial tensile strength of concrete, then the constitutive matrix in the principal directions is given by

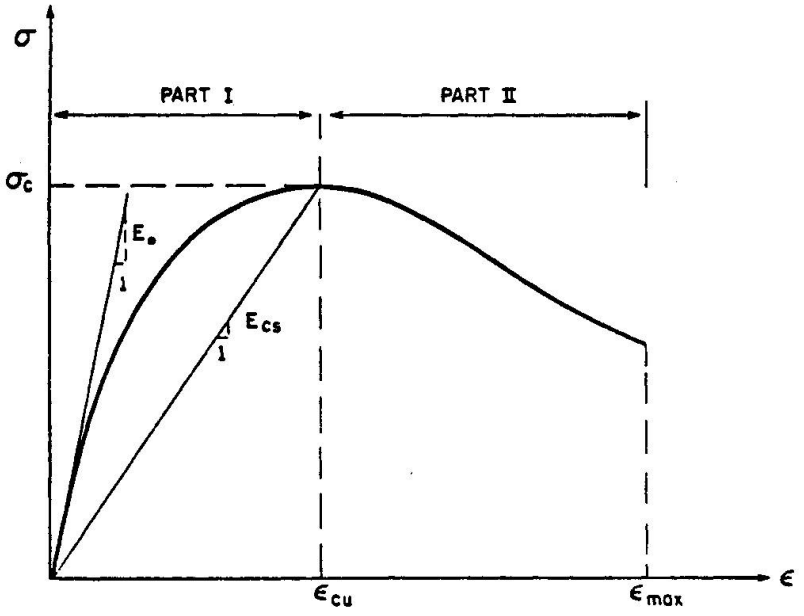

Fig. 1 - Equivalent stress-strain relation for concrete (in case of uniaxial stress $\sigma_c = f'_c$).

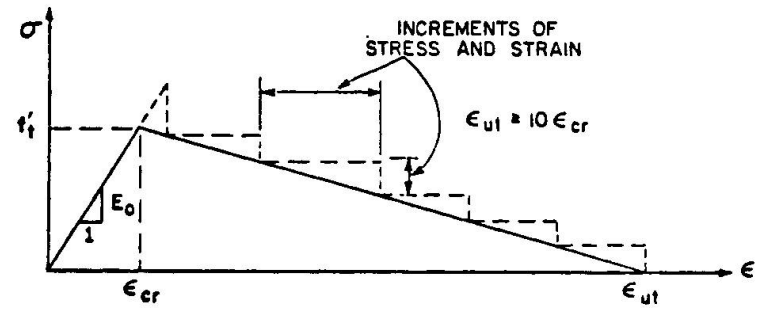

Fig. 2 - Tension stiffening model

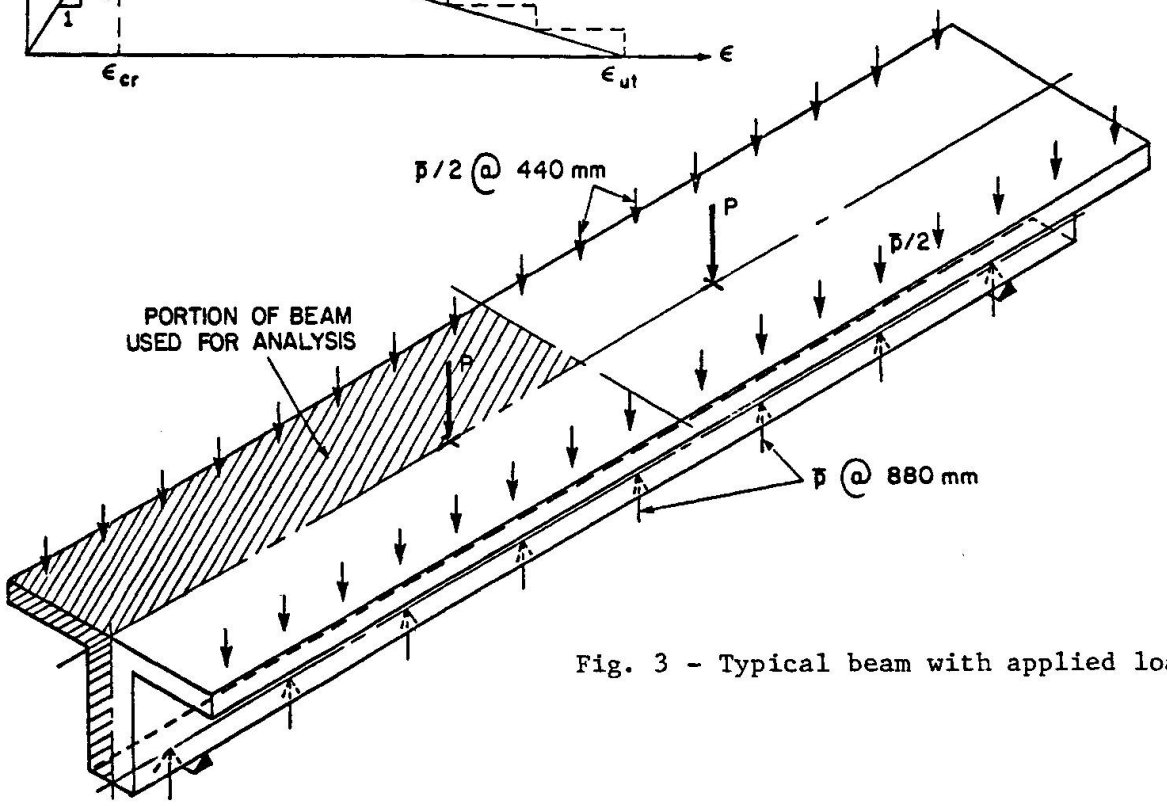

Fig. 3 - Typical beam with applied loads

$$[D] = \begin{bmatrix} 0 & 0 & 0 \\ 0 & E_2 & 0 \\ 0 & 0 & \beta G \end{bmatrix} \qquad (4)$$

while if $\sigma_1 \geq f'_t$ and $\sigma_2 \geq f'_t$, then all elements of the above matrix, except βG, are set equal to zero. In Eq. (4) G is the elastic shear modulus and β is the shear retention, or reduction, factor.

The concept of shear retention factor was first introduced by Suidan and Schnobrich [20] and later with certain modifications adopted by other analysts. In the present analysis, as demonstrated later, it was found out that setting the shear rigidity on the cracked plane equal to 10% of the uncracked concrete shear modulus, i.e. $\beta = 0.1$, and holding it constant renders good results in the case of most of the beams analyzed. In one case, however, this approach did not yield acceptable results. This will be dwelt upon in more detail later.

For accurate modelling of reinforced concrete, one has to account for the tension that is resisted by the concrete in between the cracks. This phenomenon known as "tension stiffening" is allowed for in FELARC by the use of the stress-strain relationship for concrete in tension shown in Fig. 2.

5. EXPERIMENTAL BEAMS AND THEIR ANALYTICAL MODELS

To investigate the action of longitudinal shear alone and longitudinal shear plus transverse bending at the junction of compression flange and web in reinforced concrete T-beams, Bachmann et al. [2, 3, 4, 5] carried out tests on seven beams, Fig. 3, whose transverse flange reinforcements were designed on the basis of different analyses.

Four of the above beams, namely Beams 1, 2, 4 and 7 are selected as representative. Beams 1 and 2 are intended to investigate the action of longitudinal shear alone, hence, the beam webs are loaded with two concentrated loads P at the third points of the span (Fig. 3). The amount of reinforcement running in the transverse direction in Beam 1 is determined by Bachmann et al by considering the principal stress in a longitudinal section at the intersection of the flange with the web. In Beam 2 the transverse reinforcement is designed using a spatial truss model [3, 4].

The flanges in Beams 4 and 7 are subjected to longitudinal shear and transverse bending. In addition to the concentrated loads P, a downward distributed load of $1.136\bar{p}$ per meter length is applied to the outer edges of flange. Equal and opposite forces are applied on the bottom of the web as shown in Fig. 3. The transverse flange reinforcement is obtained by superposition of required steel from the truss model for shear alone plus the steel needed for transverse bending. Beam 7 is similar to Beam 4 except that the flange is partially prestressed with a transverse prestressing of 58 kN/m. The dimensions and web reinforcement for all the beams are identical, as illustrated in Fig. 4.

Tables (1) and (2) give the concrete and steel properties data used in the analysis and were taken to comply as far as possible with data reported by Bachmann et al.

Due to symmetry about two vertical planes, only one quarter of the beams, i.e. the cross-hatched portion in Fig. 3, is analyzed. The finite element idealization of the quarter beam is shown in Fig. 5.

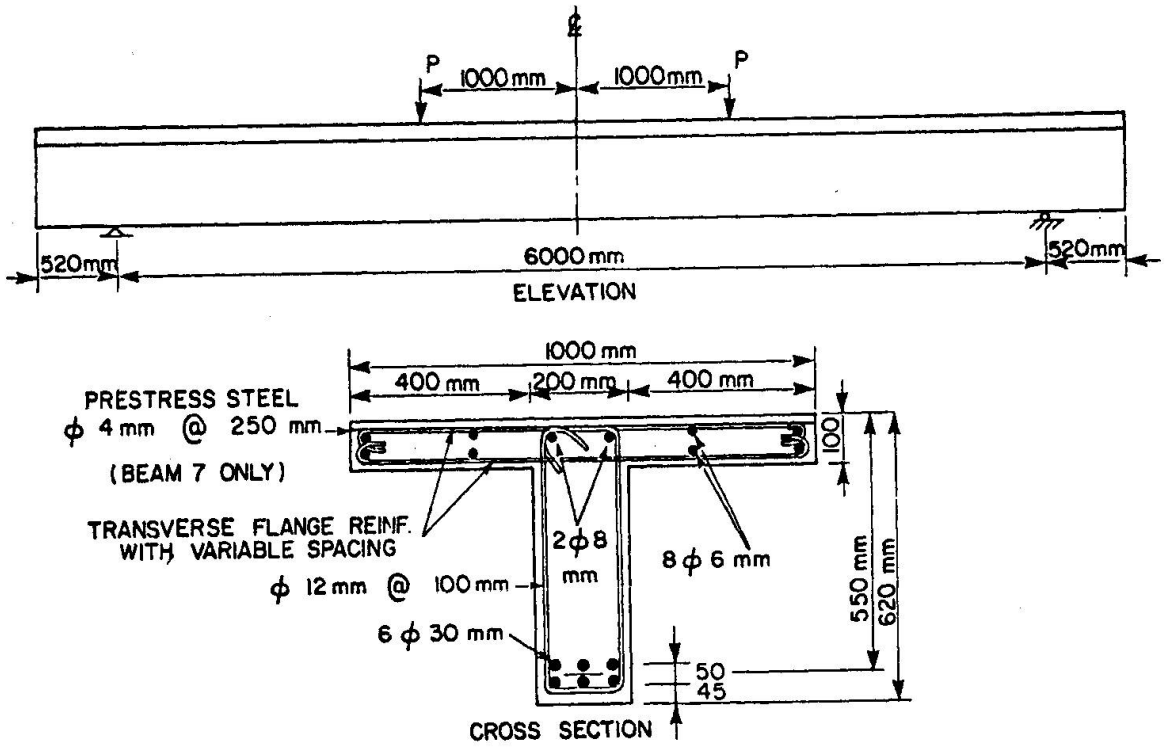

Transverse reinforcement in the flange:

Beam 1: 18 ϕ 6 mm at 85-285 mm top and bottom
Beam 2: 28 ϕ 6 mm at 125 mm top and bottom
Beam 4: 49 ϕ 6 mm at 55-100 mm top and
21 ϕ 6 mm at 125-275 mm bottom
Beam 7: 27 ϕ 6 mm at 82-250 mm top and
14 ϕ 6 mm at 275-285 mm bottom

Fig. 4 - Typical beam dimensions and reinforcement

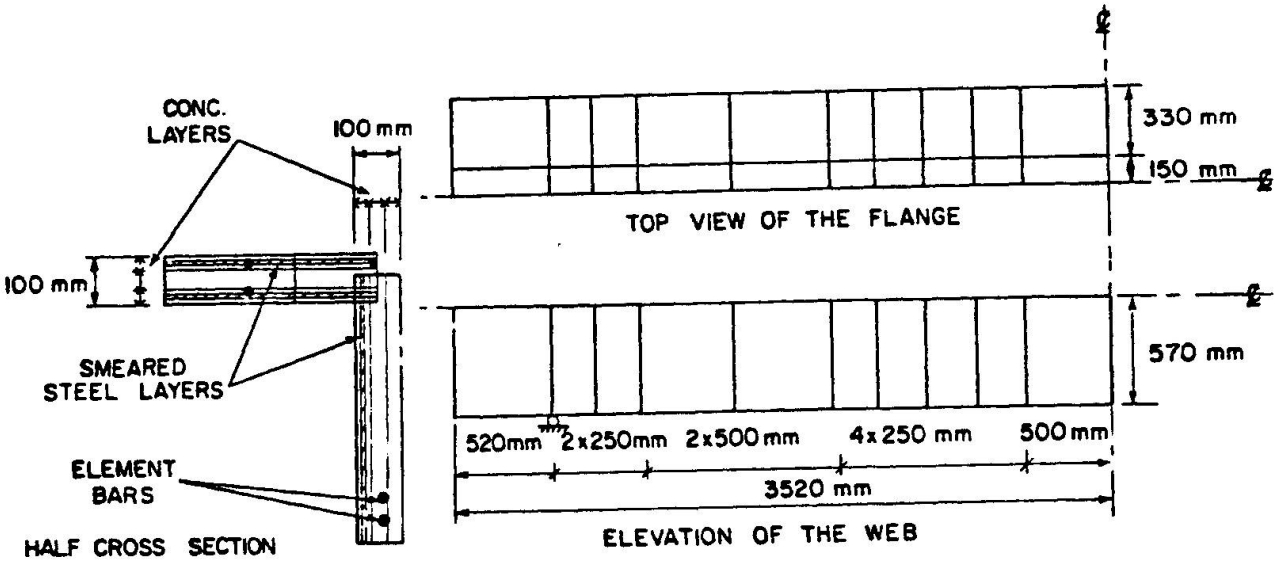

Fig. 5 - Typical finite element idealization

Table 1. Concrete strength data(1) based on 120 x 120 x 360 mm prisms

Beam No.	f'_c MPa	f'_t MPa	ε_{cu}	ε_{max}	E_o(2) GPa
1	23.40	2.16	0.00165	0.00375	31.38
2	27.22	2.45	0.00182	0.00225	34.53
4	24.71	2.06	0.00170	0.00225	34.90
7	25.57	2.26	0.00170	0.00270	34.70

(1) f'_c is the prism strength, other symbols are defined in Figs. 1 and 2.
(2) Calculated from f'_c.

Table 2. Steel strength data[1]

Bar ϕ mm	Area mm^2	f_y MPa	ε_{smax}	E_s GPa	E_s^* GPa
4	12.6	1686.63	0.037	178.3	5.31
6	28.1	482.45	0.066	196.0	0.94
12	108.0	508.93	0.162	196.0	1.16
30	696.0	567.77	0.138	196.0	1.54

(1) fy = yield stress; ε_{smax} = the strain at failure; E_s = modulus of elasticity (the value 196 MPa was assumed because it was not reported by Bachmann et al.); E_s^* = strain hardening modulus

6. RESULTS AND DISCUSSION

The load deflection curves of Beams 1, 4 and 7 are shown in Fig. 6 a to c. In all three cases analysis indicates good agreement with the load-deflection curves in the experiment but the analytical response seems slightly stiffer, especially for Beam 1. The reason may be the assumption in the analysis of higher initial concrete modulus and/or higher compressive strength. The failure loads in Table (3) corroborate this as the analysis gives 3.5 - 8% higher values. The experimental and analytical deflected shapes of Beam 4 are compared in Fig. 7 for a load of 0.76 P_u, where P_u is the failure load.

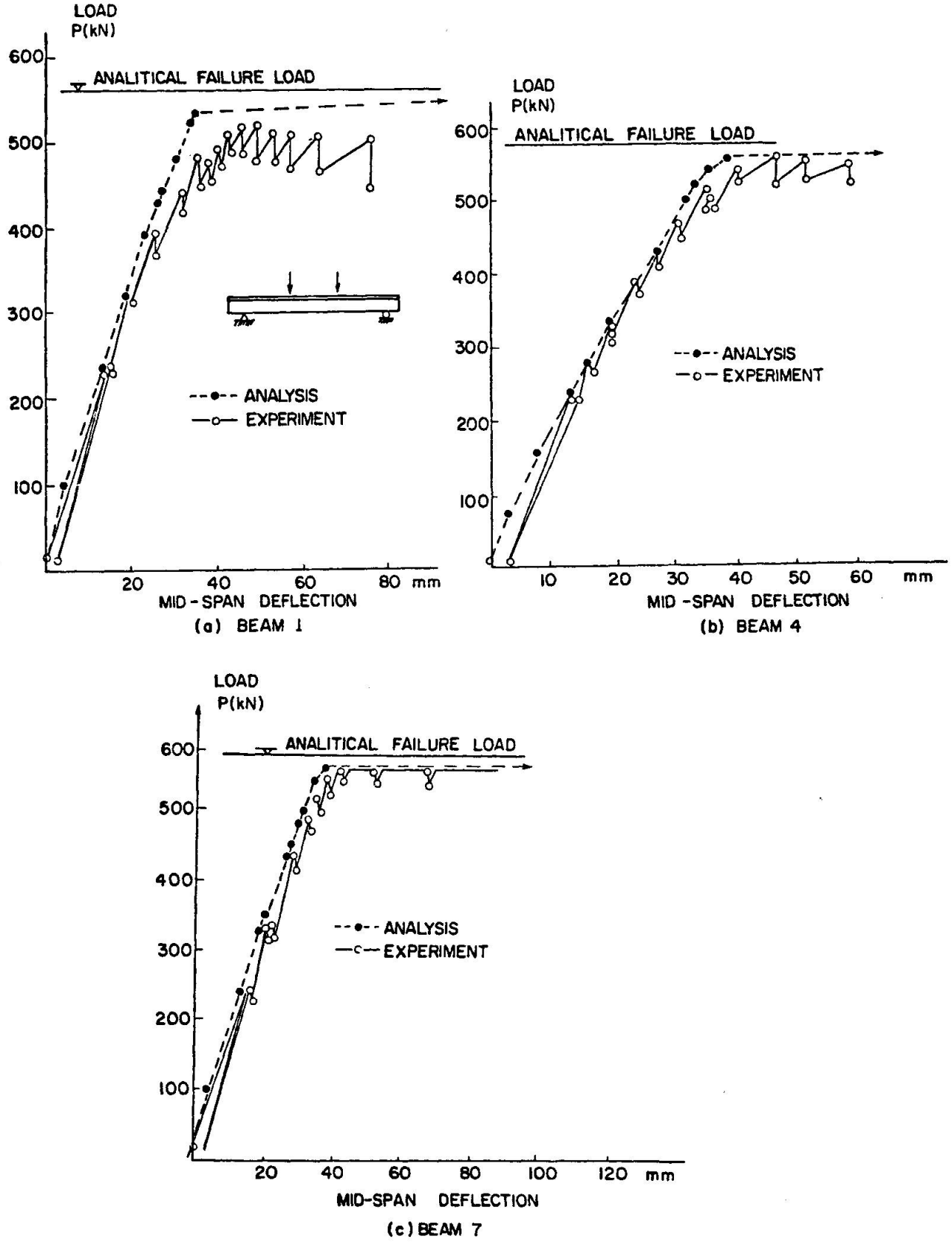

Fig. 6 - Load versus mid-span deflection

Table 3. Failure loads

Beam No.	Failure Load P_u kN		$\frac{P_u \text{ Experiment}}{P_u \text{ Analysis}}$
	Experiment	Analysis	
1	507.95	549.1	1.081
2	550.12	568.7	1.033
4	549.10	568.7	1.036
7	549.10	568.7	1.036

In Fig. 8 the strain variation in the main longitudinal web reinforcement is depicted. In the case of Beam 7, the experimental strain at P = 549.1 kN represent the failure stage, while analysis shows that failure is imminent but has not occurred yet. Therefore, unlike the experimental results, the analytical strains near the failure section are comparatively small, (Fig. 8b).

Another parameter in the analysis is the strain in concrete. Since the experimentally reported concrete strains on the top and bottom faces of the flange along the span represent average values over a base length of the instrument used (200 mm), the analytical results are also averaged from appropriate points where strains are computed. Fig. 9 illustrates the longitudinal concrete strain variation in the flanges at service and ultimate loads. The values indicated are average strains along a line at the center of the overhang. It is worthwhile to mention that since in the analysis the stiffness matrix may become singular at failure, indicating instability in the structure, the results obtained from such a load step are not generally indicative of the actual stress situation. For the analytical strains reported here, the values at 97% of P_u are considered to be the ultimate strains. This may explain the reason for the high measured strains at failure.

It is to be noted that when the flanges are subjected to transverse bending, the longitudinal strain at the top face of the flange is a shortening caused by the longitudinal bending moment of the beam as well as the shortening caused by Poisson's effect from the transverse tensile stress caused by the transverse bending of the slab in Beams 4 and 7. In the analysis Poisson's ratio is assumed constant = 0.15 while some investigators [15] observed much higher values of Poisson's ratio at stresses close to f'_c. This may account for the large discrepancy between measured and calculated strains near the center of the span for case of loading close to P_u.

7. STRAIN IN TRANSVERSE REINFORCEMENT IN THE FLANGES

Figs. 10a and b show the variation along the span of the strain in the top_ transverse steel layer for Beams 4 and 7 which are subjectd to both P and p loadings (see Fig. 3). The strains for Beams 1 and 2 are shown in Figs. 11a and b. Analytical and experimental results are reasonably close except for

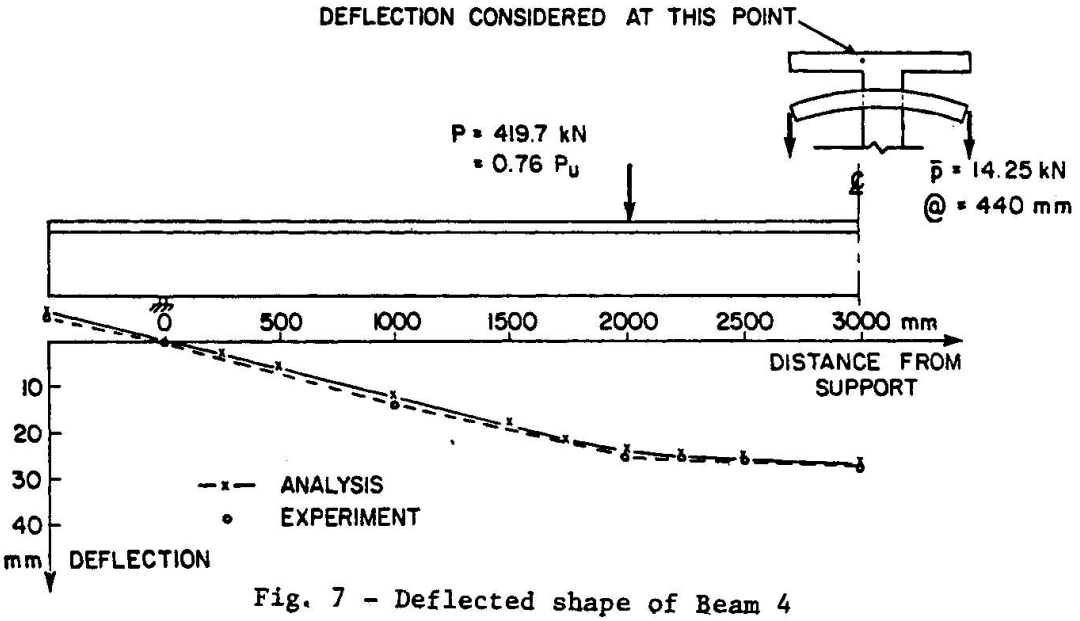

Fig. 7 - Deflected shape of Beam 4

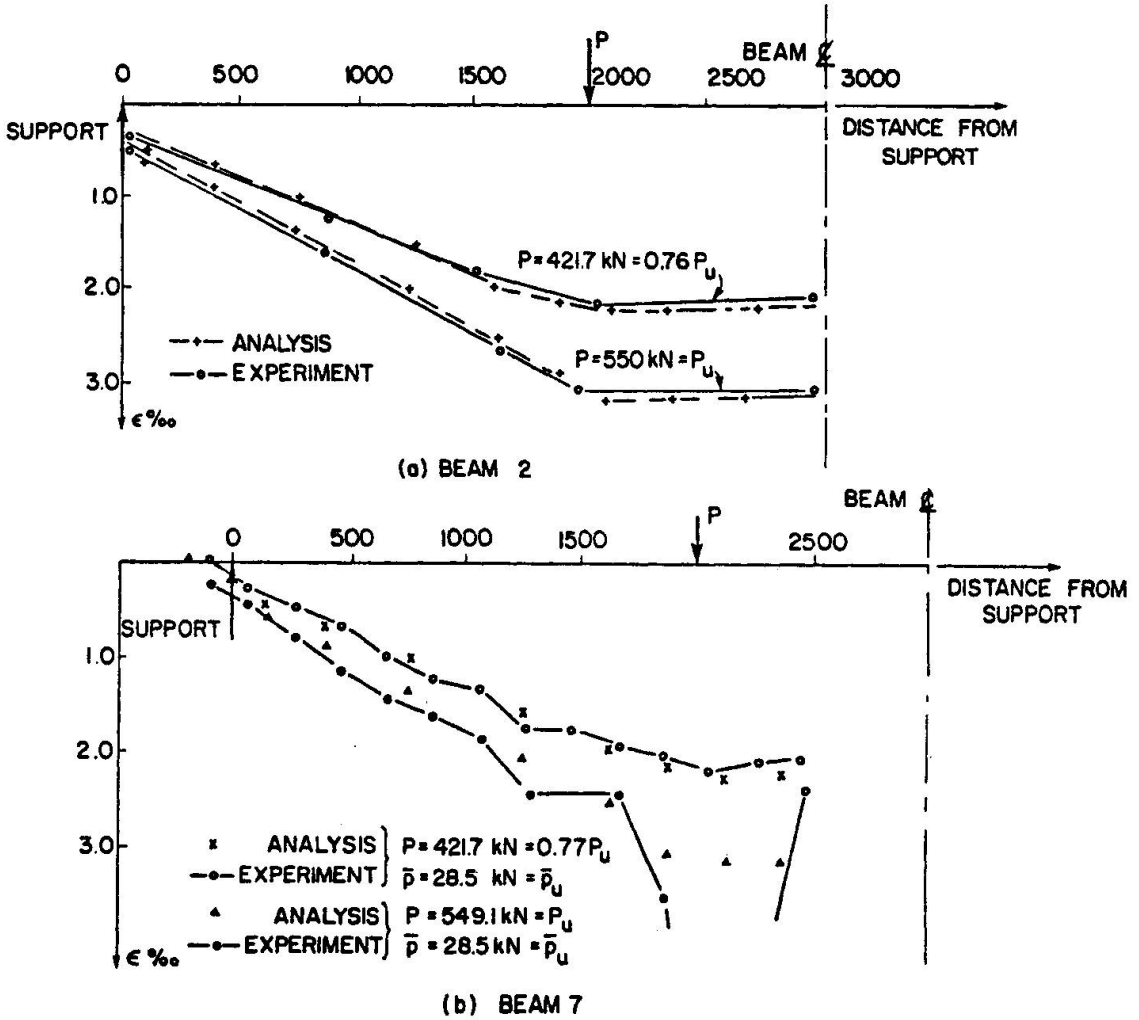

Fig. 8 - Strain in main longitudinal web reinforcement

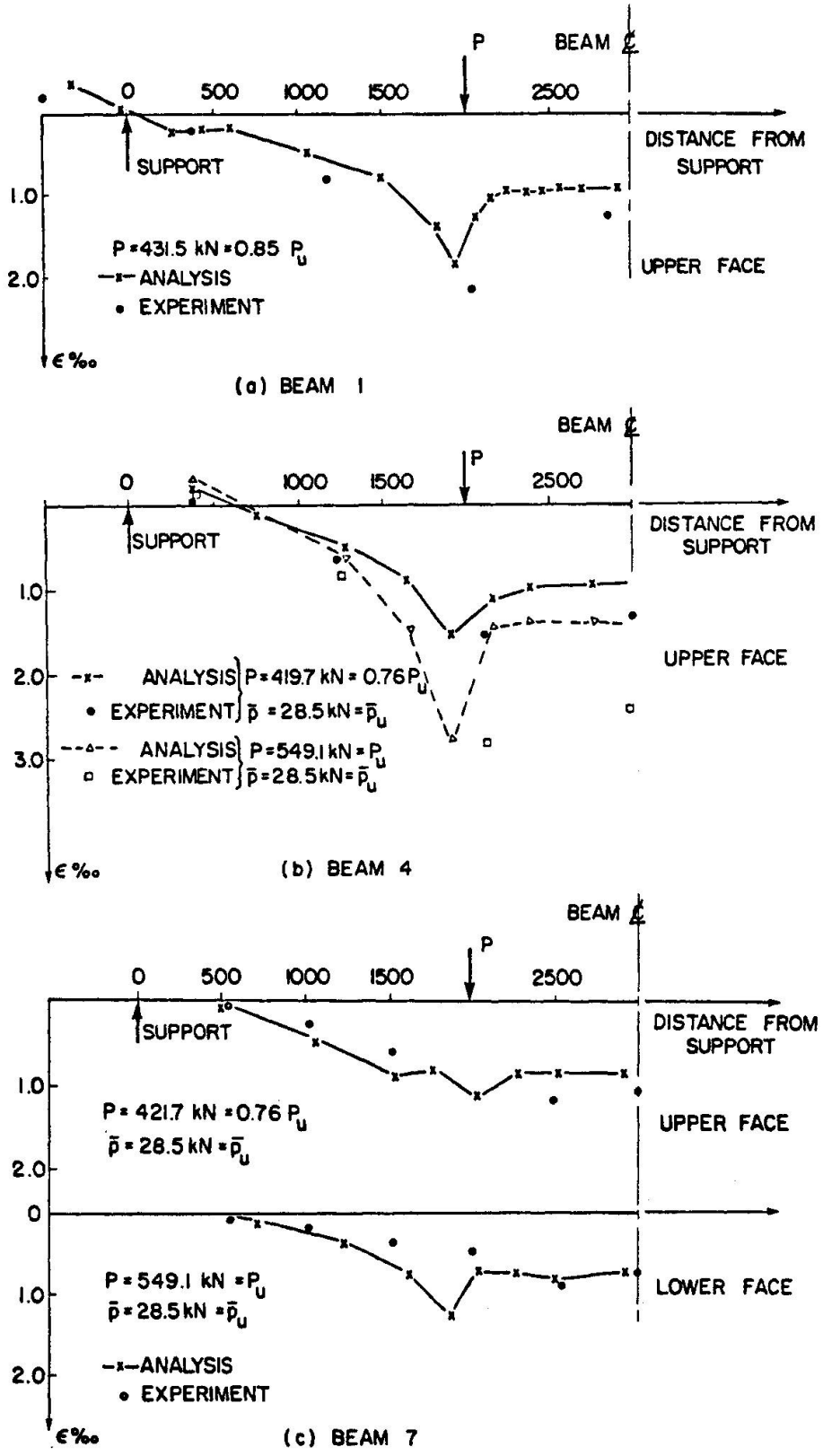

Fig. 9 - Strain in concrete in the direction of the span along centerline of the overhang

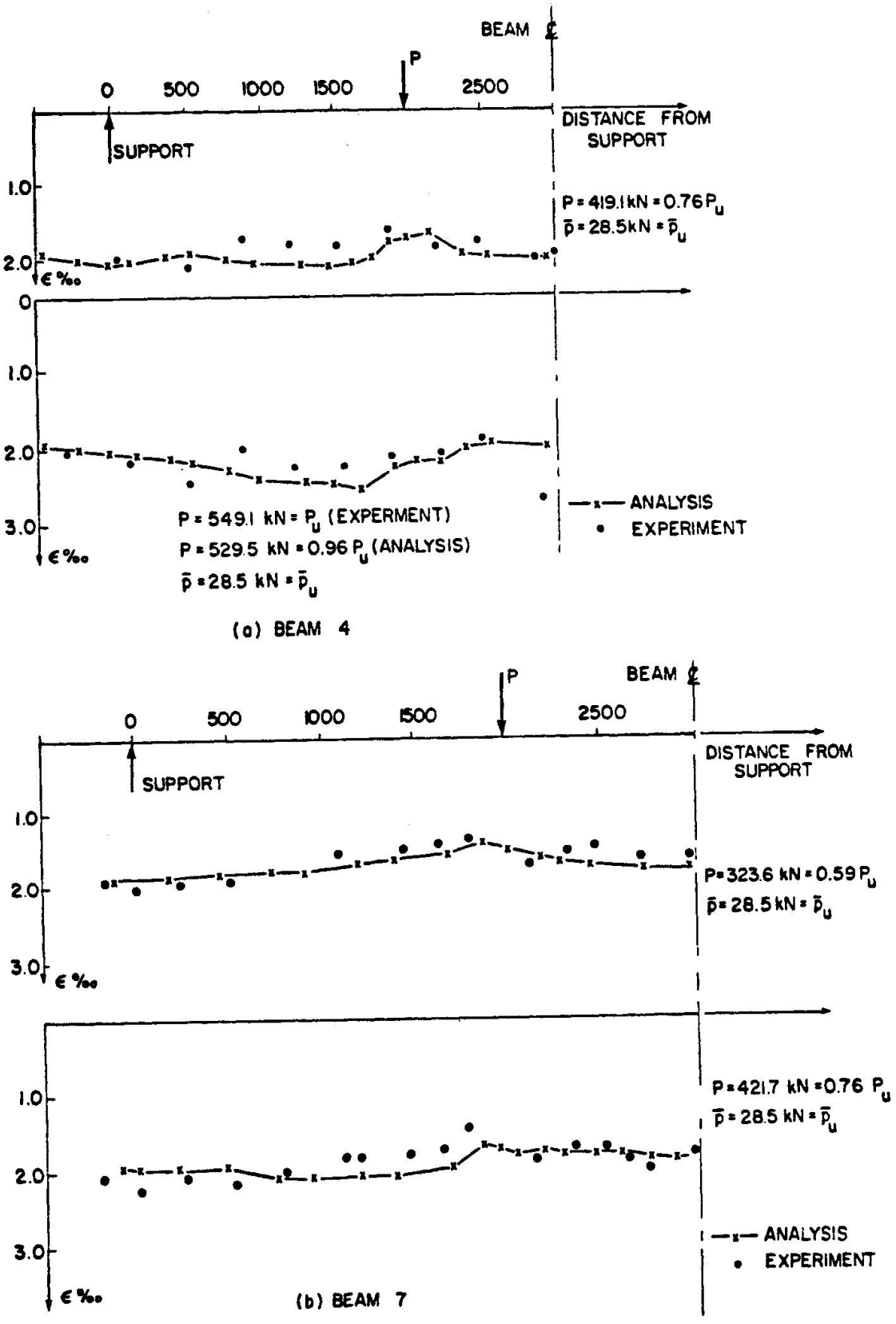

Fig. 10 - Maximum strain in transverse top reinforcement of the flange

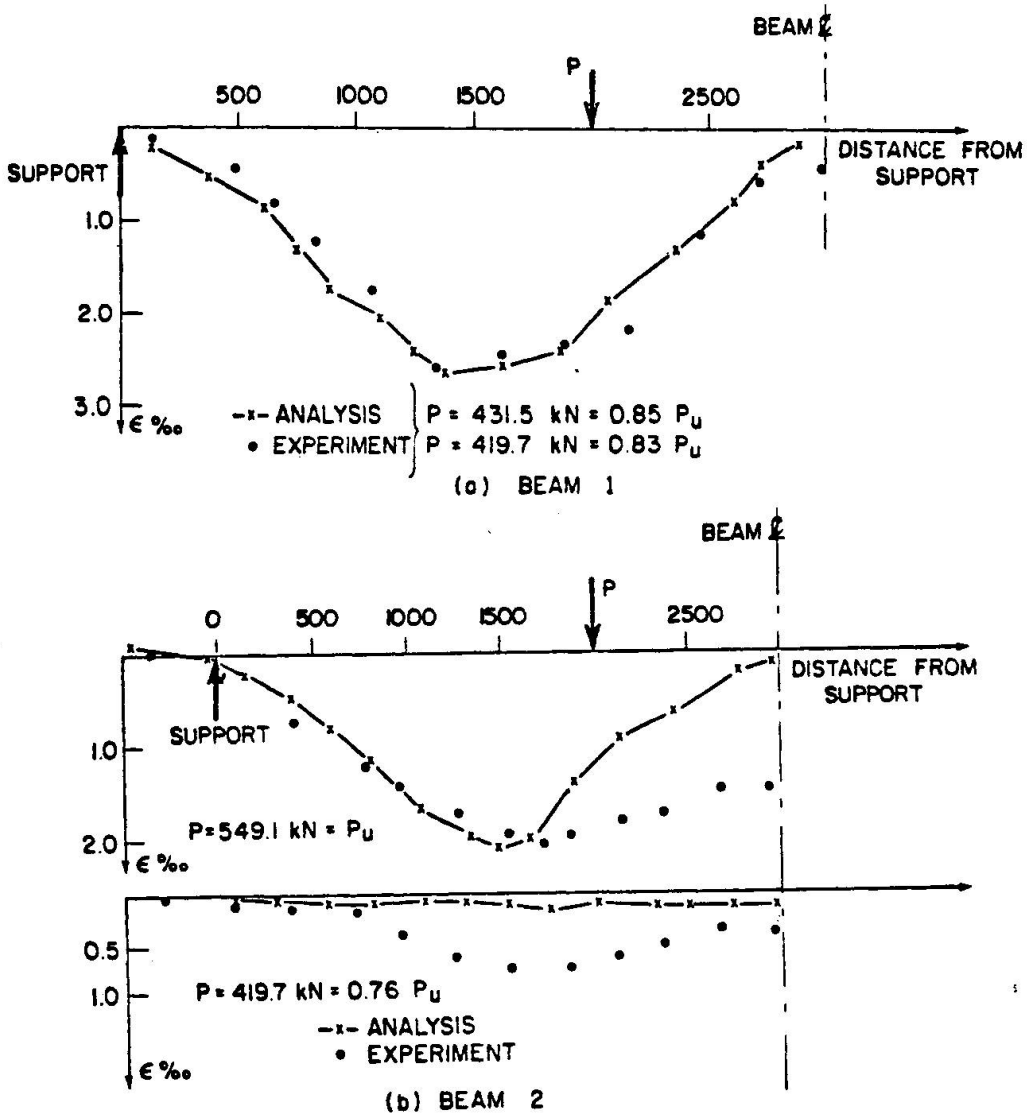

Fig. 11 - Maximum strain in transverse top reinforcement of the flange

Beam 2. This beam is not subjected to transverse bending and thus the stress in the transverse steel is caused by the longitudinal shear. Hence a close look at the way shear is accounted for in the constitutive relation used for cracked reinforced concrete, Eq. 4, is necessary. In particular, the coefficient β which accounts for the shear capacity of cracked concrete has to be examined.

Beam 2 was analyzed using successively decreasing values of β starting from 0.9. At $\beta = 0.01$, the beam failed prematurely at about $0.8\ P_u$, but varying β between these two limits had little effect on either the failure load or stress in the transverse reinforcement.

Some authors have suggested the following expressions for the reduced shear modulus $\bar{G} = \beta G$ for cracked concrete:

$$\bar{G} = 0.1E\left(1 - \frac{\varepsilon}{0.004}\right) \quad \ldots\ (a)$$

$$\bar{G} = \left(\frac{0.4\varepsilon_o}{\varepsilon}\right)G \quad \ldots\ (b)$$

$$\bar{G} = 50\left(\frac{1}{c}\right)^{1.5}\sqrt{\frac{f'_c}{34.6}} \quad \ldots\ (c)$$

$$\bar{G} = \left[\frac{1}{G} + \frac{b}{\ell(K_N + bK_D)}\right] - 1 \quad \ldots\ (d)$$

where

ε = fictitious strain normal to crack
ε_o = cracking strain
c = crack width in mm
f'_c = concrete strength in MPa
b = constant
K_N = extensional stiffness of bars crossing the crack
K_D = dowel stiffness of bars crossing the crack
ℓ = crack spacing
G = shear modulus of uncracked concrete

Expressions (b) and (a) proposed by Al-Mahaidi [1] and Cedolin and Dei Poli [7], respectively were used in the current study to analyze Beam 2 and gave results practically the same as when $\beta = 0.1$ in Eq. 4. Expression (c) suggested by Houde and Mirza [13] cannot be used unless crack widths can be determined accurately. The use of an assumed crack width in this expression will make it equivalent to (a) and (b). It is to be mentioned that expressions (a), (b) and (c) have been used, by their formulators, in conjunction with special linkage elements to account for bond stress-slip and crack opening. Since such elements would involve inclusion of additional unknown parameters they have not been adopted here.

Expression (d) was developed by Fardis and Buyukozturk [10]; and, according to its authors, applies when cracks run in one direction. This again purports knowledge of crack spacing, and gives a value of $\bar{G} = 0$ when K_N and K_D are zero (concrete without reinforcement). Such a value corresponds to $\beta = 0$.

Thus it appears that unless crack spacing is know, the more sophisticated expressions involve the same degree of approximation as the original simple approach of Suidan and Schnobrich (see Eq. 4).

Recently Bazant and Gambarova [6] and Chen and Schnobrich [8] have proposed more comprehensive models which consider crack dilatancy and crack displacement-stress non-linearity. However, while the first model still requires advance knowledge of crack spacing, the latter involves a number of constants to be determined by experiments yet to be done. Moreover both of these models are based on limited experimental data.

8. CONCLUSIONS

Four reinforced concrete T-beams that have been previously tested are analyzed by the finite element method using a non-linear iterative tangent stiffness approach. The main purpose is to study analytically the shear transfer at the web-flange connection and the interaction of this shear with transverse bending. Once an analytical procedure is established, a wide range of conditions not yet tested can be investigated.

From the study presented, it appears that although the constitutive relations for reinforced concrete used in the analytical work described in this paper, give accurate results in most situations, they are still inadequate in predicting the stress in transverse flange reinforcement in some cases. This inadequacy brings forth the exigency of developing suitable mathematical models. Such models have been recently proposed, but they require knowledge of certain parameters that are unknown a priori. Finally, it is not clear what effect geometric nonlinearity may have at later stages of loading.

ACKNOWLEDGEMENTS

The writers would like to thank Professor A. Bachman for prompt response to enquiries concerning his tests. Thanks are also due to Dr. G.A.M. Ghoneim for his assistance in the use of the computer program FELARC and to Professor W.H. Dilger for his useful discussions.

This research was supported by a grant from the Natural Sciences and Engineering Research Council of Canada which is gratefully acknowledged.

REFERENCES

[1] Al-Mahaidi, R.S.H., "Nonlinear Finite Element Analysis of Reinforced Concrete Deep Members", Report No. 79-1, Department of Structural Engineering, Cornell University, January, 1979.

[2] Bacchetta, A. and Bachmann, H., "Versuche zur teilweisen Vorspannung fur Langsschub and Querbiegung in Druckplatten von Betontragern", (Tests Concerning Partial Prestress to Resist Longitudinal Shear and Transverse Bending in Compression Flanges of Concrete Girders), Report No. 6504-9, Swiss Federal Institute of Technology, Zurich, July 1977.

[3] Bachmann, H., "Langsschub and Querbiegung in Druckplatten von Betontragern", (Longitudinal Shear and Transverse Bending in Compression Flanges of Concrete Girders), Beton-und Stahlbetonbau, Vol. 3, S. 57-63, 1978.

[4] Bachmann, H. and Bacchetta, A., "Teilweise Vorspannung fur Langsschub und Querbiegung in Druckplatten von Betontragern", (Partial Prestress to Resist Longitudinal Shear and Transverse Bending in Compression Flanges of Concrete Girders), Beton-und Stahlbetonbau, Vol. 5, S. 116-120, 1978.

[5] Badawy, M. and Bachmann, H., "Versuche uber Langsschub und Querbiegung in Druckplatten von Betontragern", (Tests Concerning longitudinal Shear and Transverse Bending in Compression Flanges of Concrete Girders), Report No. 6504-8, Swiss Federal Institute of Technology, Zurich, June 1977.
[6] Bazant, Z.P. and Gambarova, P., "Rough Cracks in Reinforced Concrete", Proceedings, ASCE, Vol. 106, No. ST4, April 1980.
[7] Cedolin, L. and Dei Poli, S., "Finite Element Studies of Shear-Critical R/C Beams", Proceedings, ASCE, Vol. 103, No. EM3, June 1977.
[8] Chen, E.Y. and Schnobrich, W., "Models for the Post-Cracking Behavior of Plain Concrete under Short Term Montonic Loading", Proc. NASA Conf. on Research in Nonlinear Structural and Solid Mechanics, Washington D.C., October 1980.
[9] Darwin, D. and Pecknold, D.A., "Nonlinear Biaxial Stress-Strain Law for Concrete", Proceedings, ASCE, Vol. 103, No. EM4, April 1977
[10] Fardis, N.M. and Buyukozturk, O., "Shear Stiffness of Concrete by Finite Elements", Proceedings, ASCE, Vol. 106, No. St6, June 1980.
[11] Ghoneim, G.A.M., "Nonlinear Analysis of Concrete Structures", Ph.D. Thesis, Department of Civil Engineering, The University of Calgary, Canada, August 1978.
[12] Ghoneim, G.A.M. and Ghali, A., "Users Manual for Computer Program FELARC (Finite Element Layered Analysis of Reinforced Concrete), Report No. CE78-15, Department of Civil Engineering, The University of Calgary, Canada, May 1979.
[13] Houde, J. and Mirza, M.S., "A Finite Element Analysis of Shear Strenth of Reinforced Concrete Beams", ACI, SP 42, 1974.
[14] Kupfer, H.B. and Gerstle, K.H., "Behavior of Concrete under Biaxial Stresses", Proceedings, Vol. 99, No. EM4, August 1973.
[15] Kupfer, H., Hilsdorf, H.K. and Rusch, H., "Behavior of Concrete under Biaxial Stresses", ACI Journal, Proc. Vol. 66, No. 8, August 1969.
[16] Ngo, D. and Scordelis, A.C., "Finite Element Analysis of Reinforced Concrete Beams", ACI Journal, Proc. Vol. 64, No. 3, March 1967.
[17] Saenz, L.D., Disc. of "Equation for the Stress-Strain Curve of Concrete, by Desayi and Krishnan, ACI Journal, Proc. No. 61, No. 9, September 1964.
[18] Sisodiya, R.G. and Ghali, A., "Analysis of Box Girder Bridges of Arbitrary Shape", Publications, IABSE, Vol. 33-I, 1973, pp. 203-218.
[19] Smith, G.M. and Young, L.E., "Ultimate Theory in Flexure by Exponential Function", ACI Journal, Vol. 52, No. 3, November 1955.
[20] Suidan, M. and Schnobrich, W.C., "Finite Element Analysis of Reinforced Concrete", Proceedings, ASCE, Vol. 99, No. ST10, October 1973
[21] Zienkiewiez, O.C., "The Finite Element Method", 3rd Ed. McGraw-Hill, London, 1977, (pp. 234-241).